Deep Space Exploration Society

A Non-Profit Corporation Dedicated to the Excitement of Hands-on Space Exploration

# Science Meeting
# May 20, 2019

**Dr. Richard Russel**

DSES.science

# Pulsar Galactic Navigation

- Pulsar Basics
- Galactic Path Planning
- Pulsar visibility along path
- Pulsar base period
- ATNF and SIMBAD database
- Pulsar simulator
- The use of Excel Solver to solve 3-dimensional galactic solution
- Selecting pulsars for navigation
- Solving Galactic Position based on pulsar observations

# Pulsar Basics

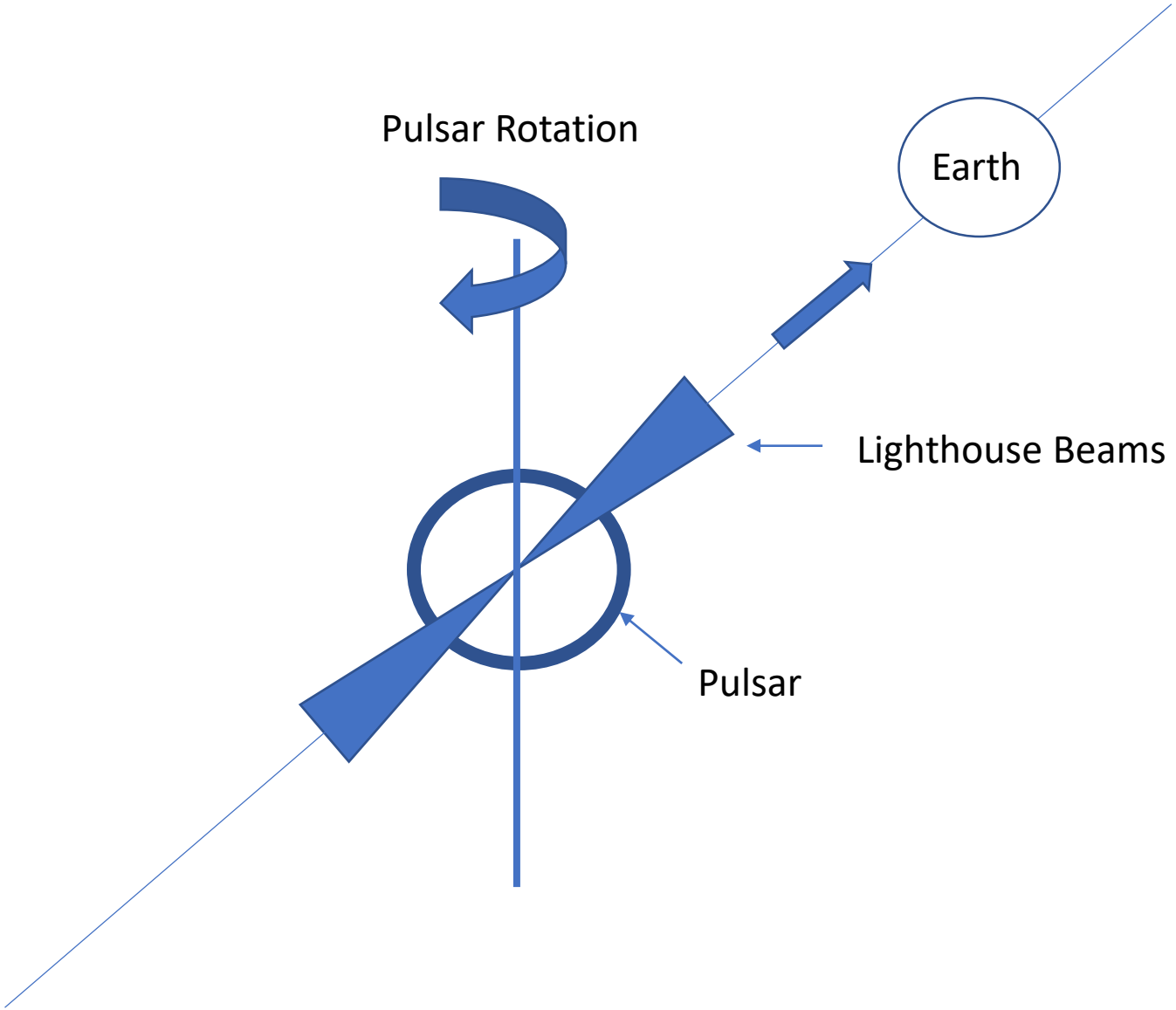

# Pulsar P-Pdot Map

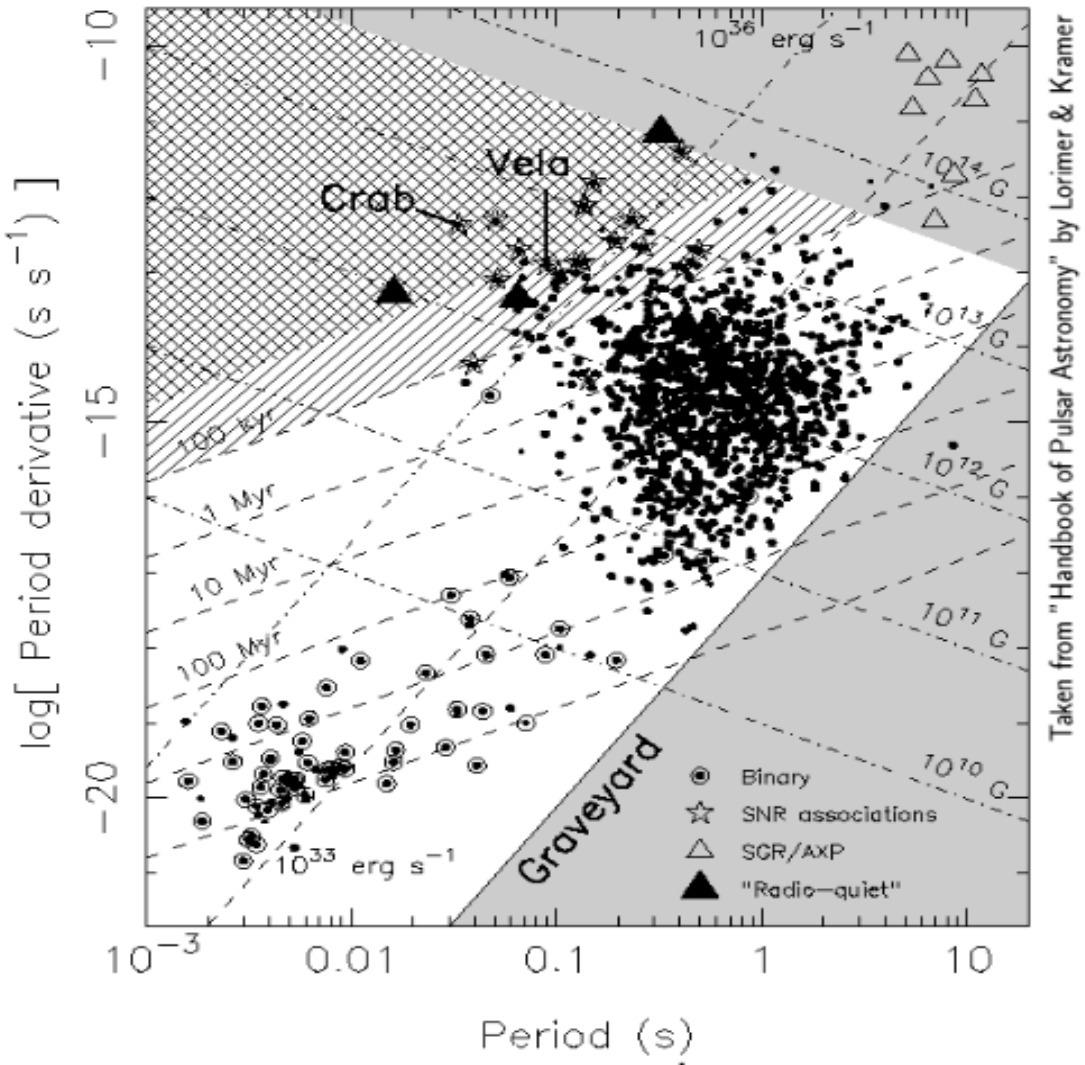

# Pulsar Geometry

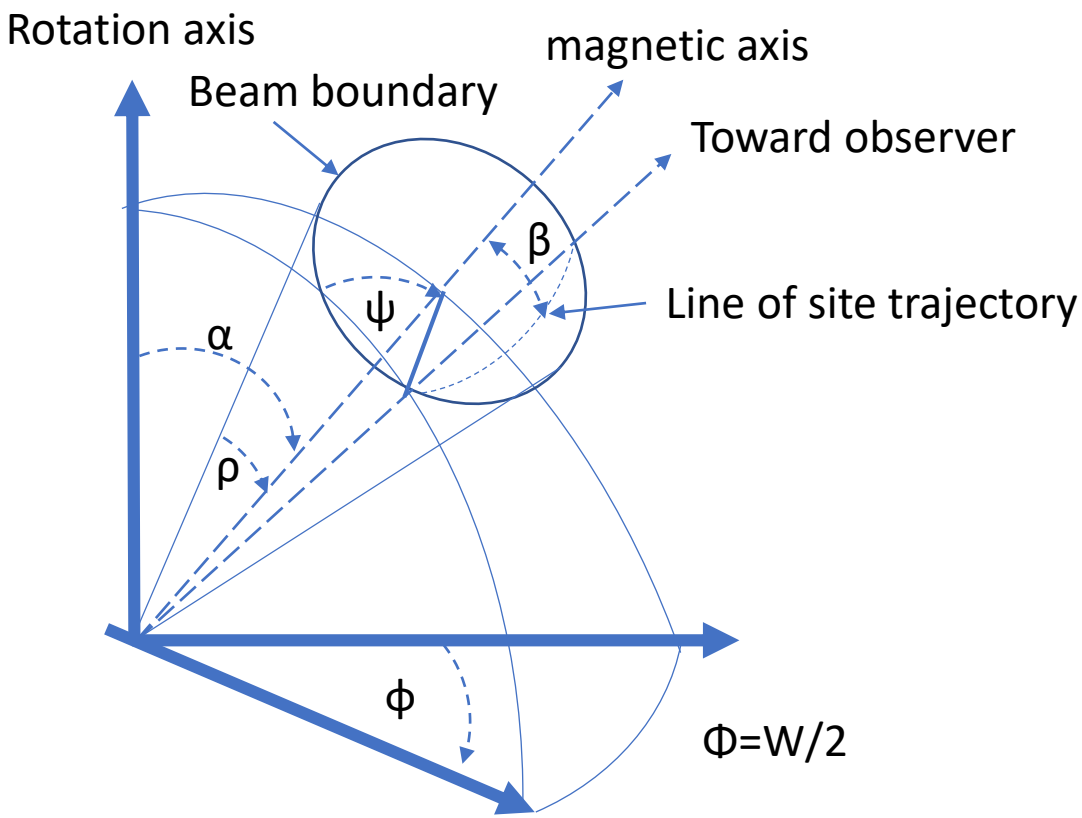

# Galactic Path Model

| | Gal-X (pc) (Galactic-Centric) | Gal-Y (pc) (Galactic-Centric) | Gal-Z (pc) (Galactic-Centric) |
|---|---|---|---|
| Earth | 0.00 | 8500.00 | 0.00 |
| 25% | 103.47 | 8477.75 | 18.64 |
| 50% | 206.94 | 8455.50 | 37.28 |
| 75% | 310.41 | 8433.25 | 55.92 |
| K452b | 413.89 | 8411.00 | 74.55 |

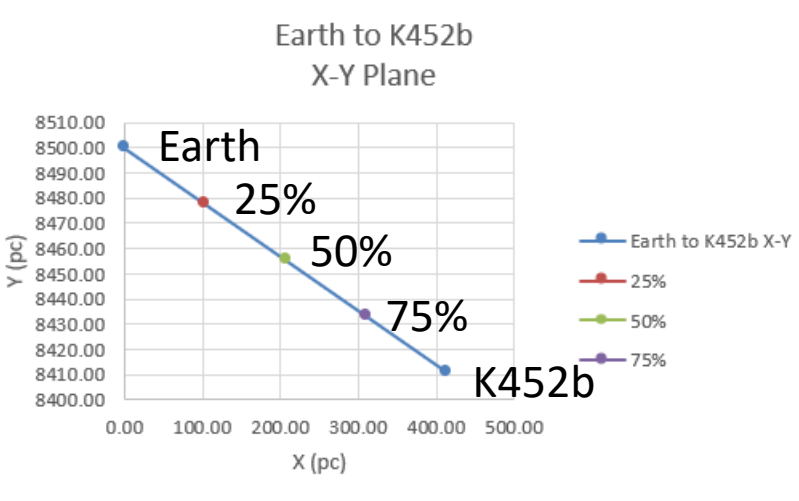


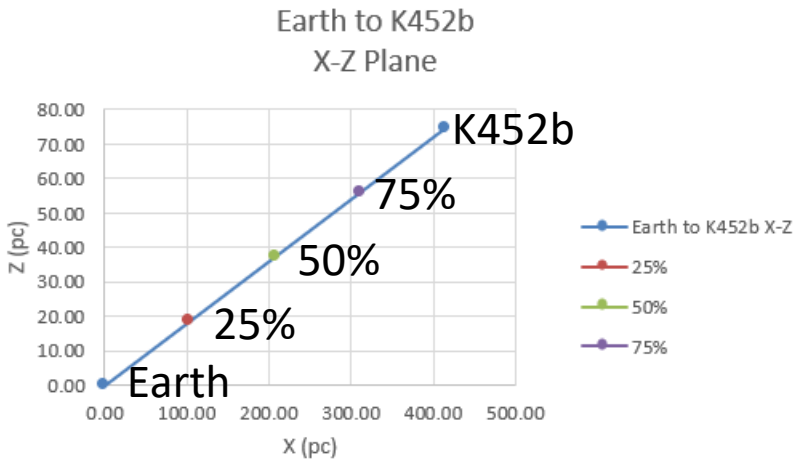


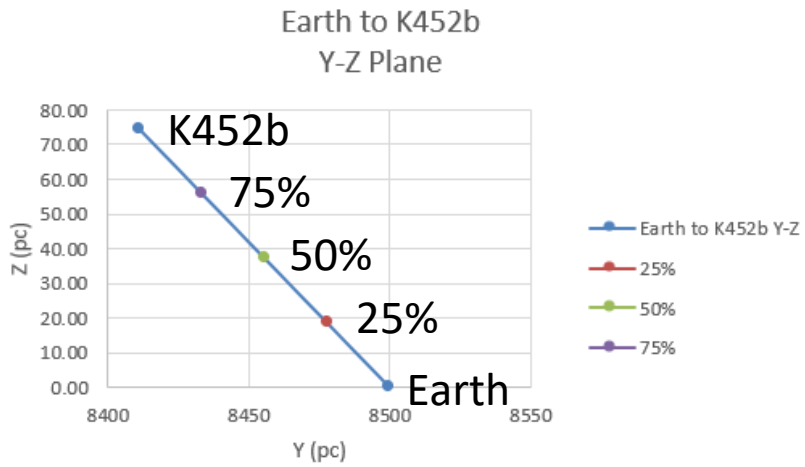

# Pulsar Observations Along Travel Path

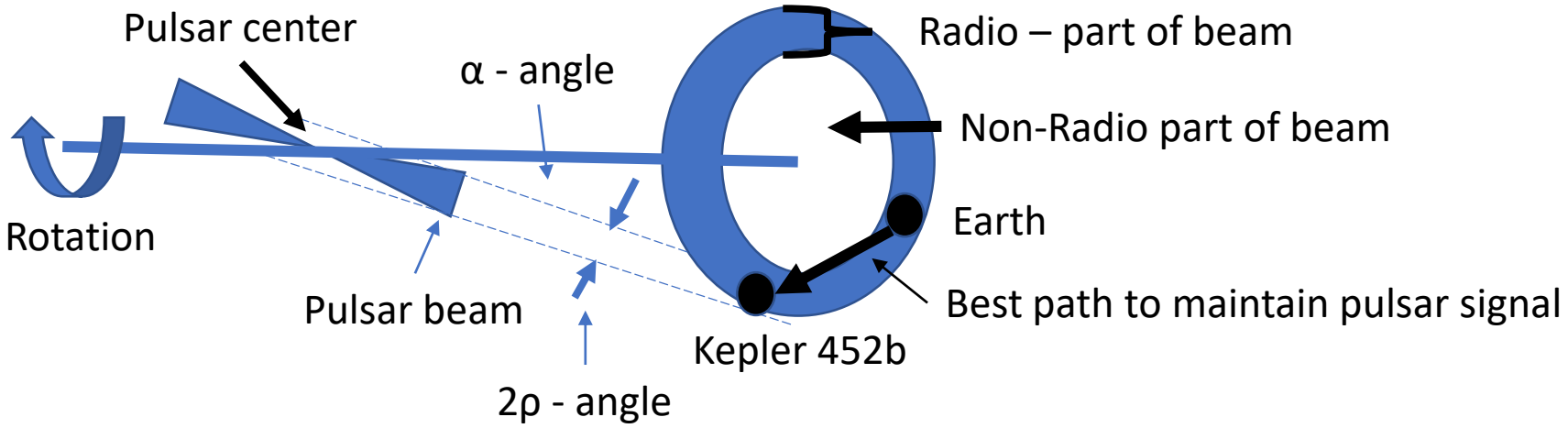

# Sources of Pulsar Data

## ATNF Database

www.atnf.csiro.au


| # | PSRJ | | Gl (deg) | Gb (deg) | P0 (s) | | | P1 | | | DIST (kpc) |
|---|---|---|---|---|---|---|---|---|---|---|---|
| 1 | J0002+6216 | cwp+17 | 117.327 | -0.074 | 0.1153635682680 | 14 | cwp+17 | 5.96703E-15 | 7 | cwp+17 | * |
| 2 | J0006+1834 | cnt96 | 108.172 | -42.985 | 0.69374767047 | 14 | cn95 | 2.097E-15 | 12 | cn95 | 0.86 |
| 3 | J0007+7303 | aaa+09c | 119.660 | 10.463 | 0.3158731909 | 3 | awd+12 | 3.6039E-13 | 5 | awd+12 | 1.40 |
| 4 | J0011+08 | dsm+16 | 106.228 | -53.407 | 2.55287 | 0 | dsm+16 | * | 0 | * | 5.40 |
| 5 | J0014+4746 | dth78 | 116.497 | -14.631 | 1.240699038946 | 11 | hlk+04 | 5.6446E-16 | 14 | hlk+04 | 1.78 |
| 6 | J0023+0923 | hrm+11 | 111.383 | -52.849 | 0.003050203104480002 | 7 | abb+18 | 1.14234E-20 | 4 | abb+18 | 1.11 |
| 7 | J0024-7204aa | phl+16 | 305.895 | -44.889 | 0.00184 | 0 | phl+16 | * | 0 | * | 2.69 |
| 8 | J0024-7204ab | phl+16 | 305.891 | -44.891 | 0.0037046394947985 | 6 | frk+17 | 9.820E-21 | 9 | frk+17 | 2.54 |
| 9 | J0024-7204C | mld+90 | 305.923 | -44.892 | 0.00575677999551635 | 14 | frk+17 | -4.98503E-20 | 20 | frk+17 | 4.69 |
| 10 | J0024-7204D | mlr+91 | 305.881 | -44.893 | 0.00535757328486573 | 9 | frk+17 | -3.4220E-21 | 9 | frk+17 | 4.69 |
| 11 | J0024-7204E | mlr+91 | 305.883 | -44.883 | 0.00353632915276244 | 4 | frk+17 | 9.85103E-20 | 6 | frk+17 | 4.69 |
| 12 | J0024-7204F | mlr+91 | 305.899 | -44.892 | 0.00262357935251262 | 4 | frk+17 | 6.45029E-20 | 7 | frk+17 | 4.69 |
| 13 | J0024-7204G | rlm+95 | 305.891 | -44.893 | 0.00404037914356515 | 14 | frk+17 | -4.21584E-20 | 17 | frk+17 | 4.69 |
| 14 | J0024-7204H | mlr+91 | 305.896 | -44.902 | 0.00321034070935032 | 11 | frk+17 | -1.8294E-21 | 11 | frk+17 | 4.69 |
| 15 | J0024-7204I | mlr+91 | 305.892 | -44.893 | 0.00348499206166289 | 13 | frk+17 | -4.5874E-20 | 3 | frk+17 | 4.69 |
| 16 | J0024-7204J | mlr+91 | 305.909 | -44.903 | 0.00210063354535246 | 5 | frk+17 | -9.7917E-21 | 9 | frk+17 | 4.69 |

## SIMBAD Database

http://simbad.u-strasbg.fr/simbad/

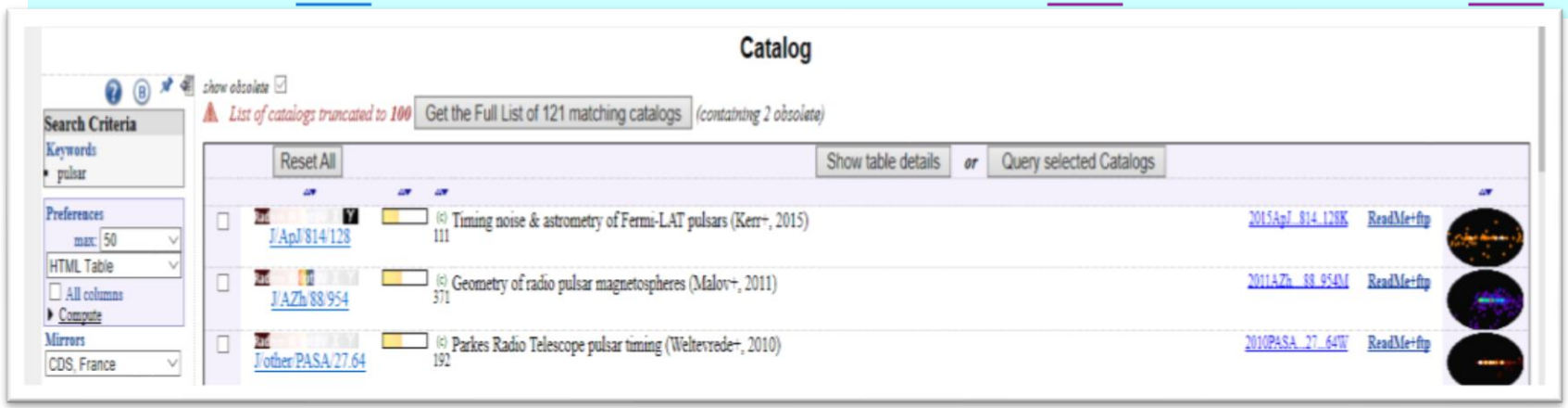

# Path Angles to Pulsar

Galactic X-Y Plane

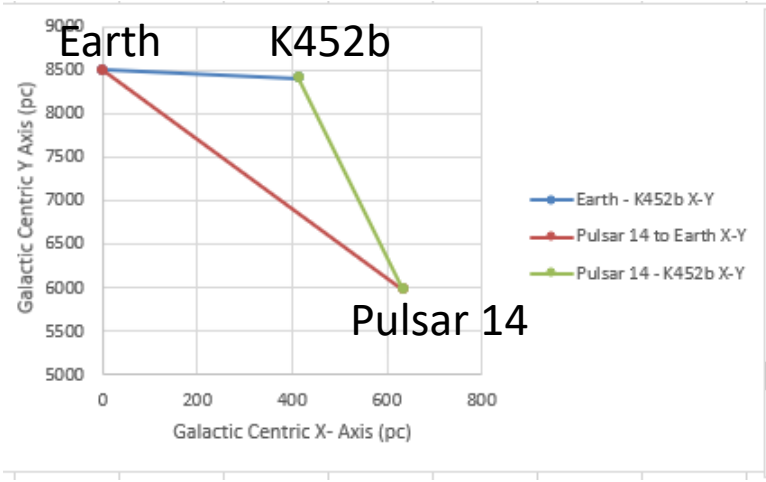


Galactic X-Z Plane

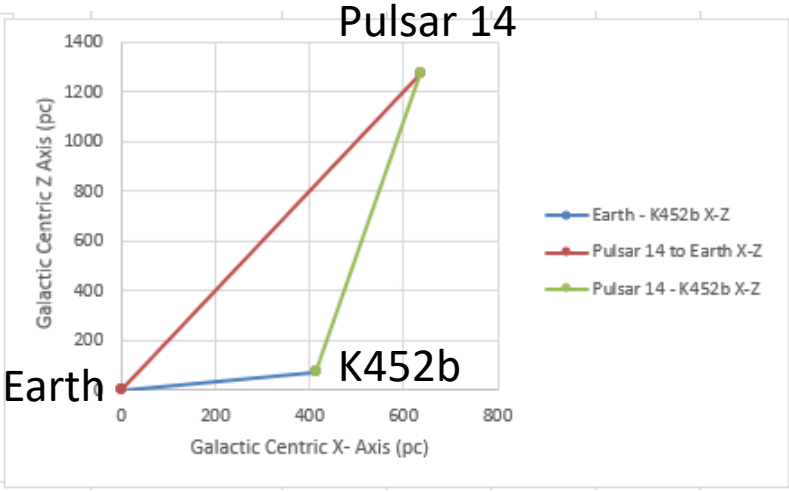


Galactic Y-Z Plane

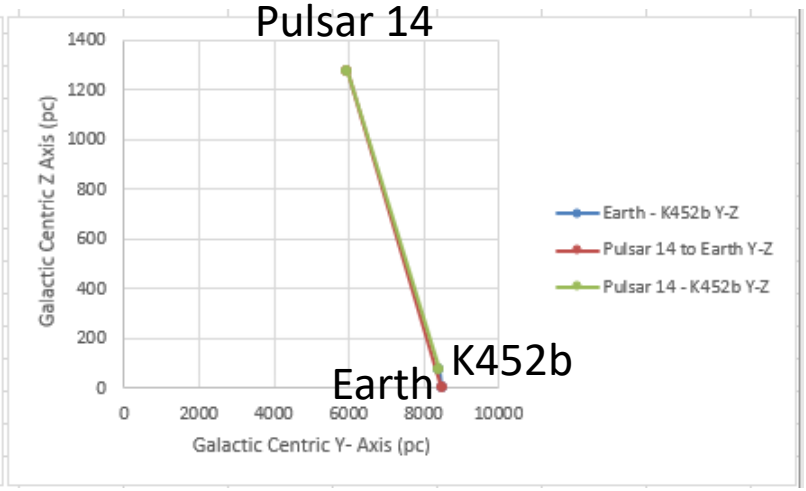

# Finding Angles

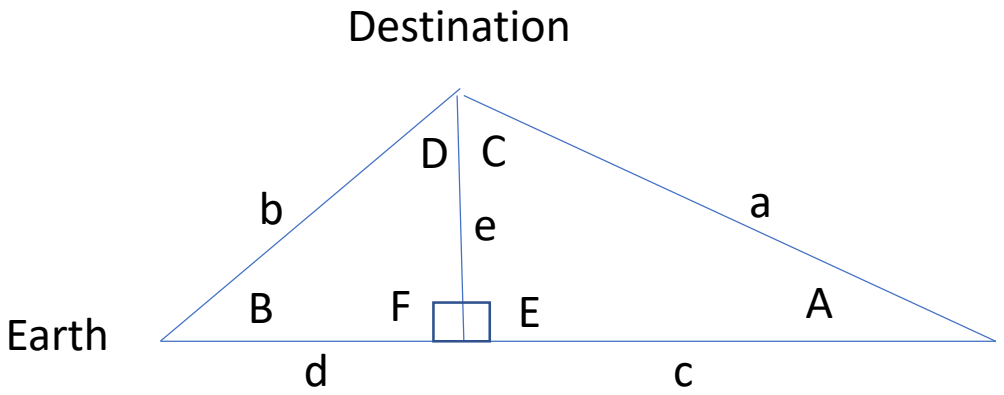


a: Pulsar to Destination Distance – known
b: Earth to Destination Distance – known
c+d: Earth to Pulsar Distance – known
e: Base Height
A: Earth – Pulsar - Destination Angle – unknown
B: Pulsar –Earth –Destination Angle – unknown
C+D: Pulsar – Destination –Earth Angle - unknown
E & F: 90 degree Angles by definition

$$\frac{c+d}{a}=\frac{a}{c}$$ P 105 Geometry Cliff Notes

$c=\frac{a^2}{c+d}$

d= (c+d)-c

$e=\sqrt{|a^2-c^2|}$

A= $ASIN\left(\frac{e}{a}\right)$

B= $ACOS\left(\frac{d}{b}\right)$

C= $ASIN\left(\frac{c}{a}\right)$

D= $ASIN\left(\frac{d}{b}\right)$

# Can the Pulsar be seen on path?

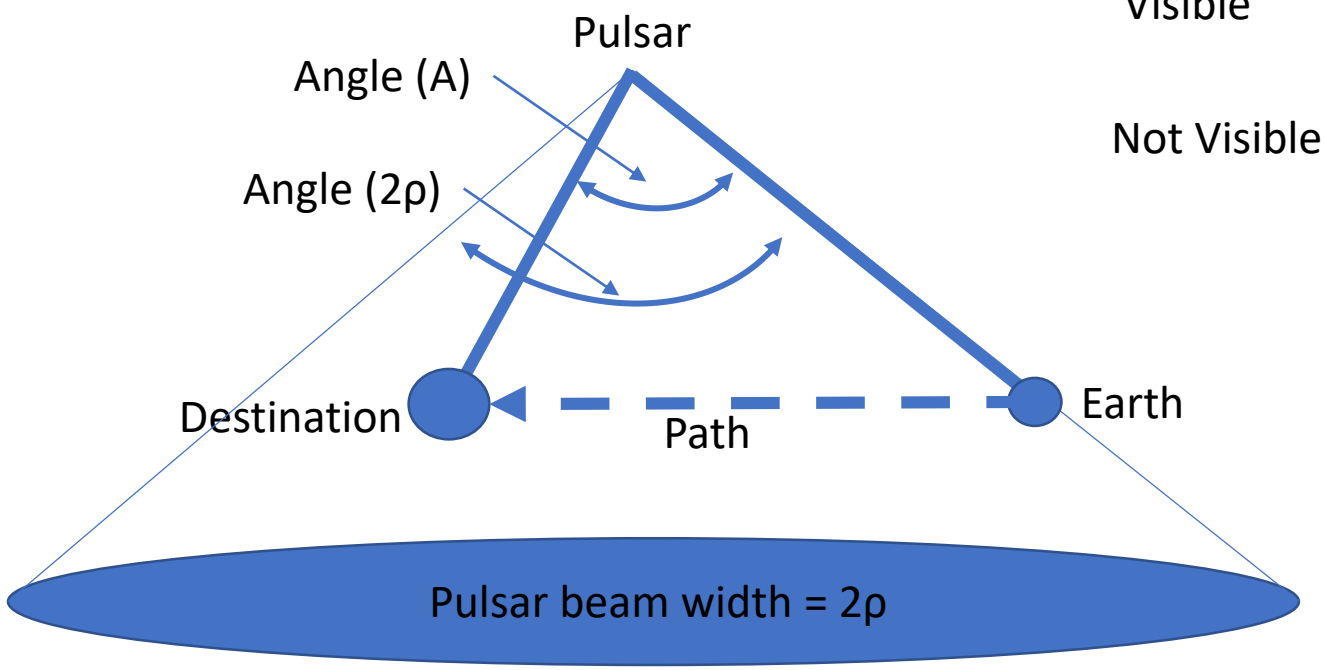


Visible — Angle (A) ≤ Angle (2ρ)

Not Visible — Angle (A) > Angle (2ρ)

Relationship needs to be true for X-Y, X-Z and Y-Z planes

Assumption is that Earth is on edge of beam

If not there is less pulsar beam width to be visible along path

# Model to Calculate Galactic Angles

Angle is between Minimum and Maximum

α±ρ angle

| | X | Y | Z |
|---|---|---|---|
| Earth | 0.0 | 8500.0 | 0.0 |
| 100% | 413.9 | 8411.0 | 74.6 |
| K452b | 413.9 | 8411.0 | 74.6 |
| Pulsars | | | |
| 0006+1834 | 486.5 | 8659.7 | -477.3 |
| 0006+1834 | 597.8 | 8696.2 | -586.3 |
| 0218+4232 | 3622.3 | 12742.4 | -1761.7 |
| 0014+4746 | 1593.3 | 9294.3 | -464.8 |
| 1857+0943 | 604.7 | 7835.2 | 48.1 |
| 2037+1942 | 1784.9 | 7597.5 | -449.7 |
| 2205+1444 | 2716.5 | 7715.2 | -1758.9 |
| 2242+6950 | 2098.8 | 9357.4 | 387.3 |

| X-Y Earth to Pulsar | X-Y Earth to Path % | X-Y Pulsar to Path % | X-Y Angle | X-Z Earth to Pulsar | X-Z Earth to Path % | X-Z Pulsar to Path % | X-Z Angle | Y-Z Earth to Pulsar | Y-Z Earth to Path % | Y-Z Pulsar to Path % | X-Z Angle |
|---|---|---|---|---|---|---|---|---|---|---|---|
| 512.1 | 423.3 | 259.1 | 55.8 | 881.5 | 420.5 | 556.6 | 38.1 | 503.3 | 116.1 | 605.3 | 13.3 |
| 629.2 | 423.3 | 339.4 | 42.3 | 837.3 | 420.5 | 686.0 | 30.1 | 618.3 | 116.1 | 719.8 | 10.8 |
| 5578.4 | 423.3 | 5390.2 | 4.4 | 4028.0 | 420.5 | 3696.7 | 6.0 | 4593.6 | 116.1 | 4704.5 | 1.4 |
| 1780.3 | 423.3 | 1473.5 | 13.8 | 1659.7 | 420.5 | 1296.9 | 14.7 | 920.3 | 116.1 | 1034.9 | 7.2 |
| 898.7 | 423.3 | 606.6 | 28.1 | 606.6 | 420.5 | 192.7 | 43.9 | 666.6 | 116.1 | 576.4 | 10.0 |
| 2000.1 | 423.3 | 1594.2 | 12.2 | 1840.7 | 420.5 | 1467.8 | 13.2 | 1008.3 | 116.1 | 967.8 | 6.6 |
| 2827.5 | 423.3 | 2405.4 | 8.6 | 3236.2 | 420.5 | 2943.4 | 7.5 | 1926.1 | 116.1 | 1961.1 | 3.5 |
| 2267.2 | 423.3 | 1932.5 | 10.8 | 2134.2 | 420.5 | 1713.7 | 11.4 | 940.8 | 116.1 | 996.7 | 7.1 |

| Alpha | rho (p) | Min | Max |
|---|---|---|---|
| 10 | 20 | -10 | 30 |

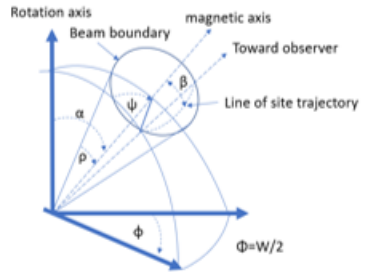


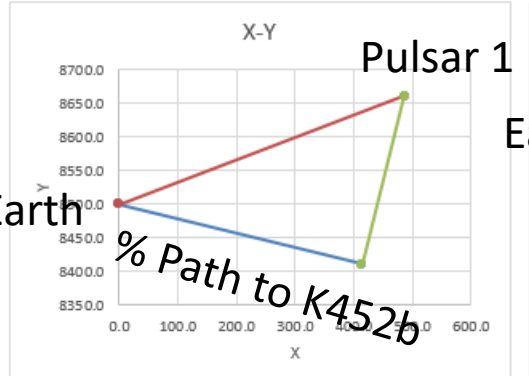


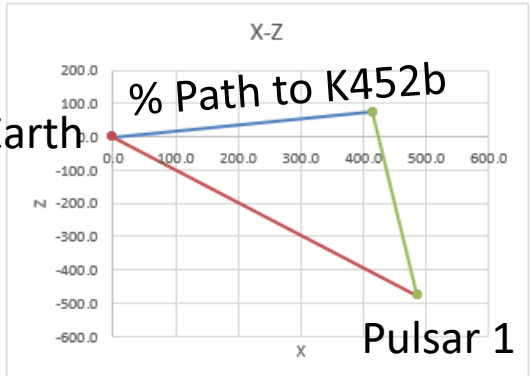


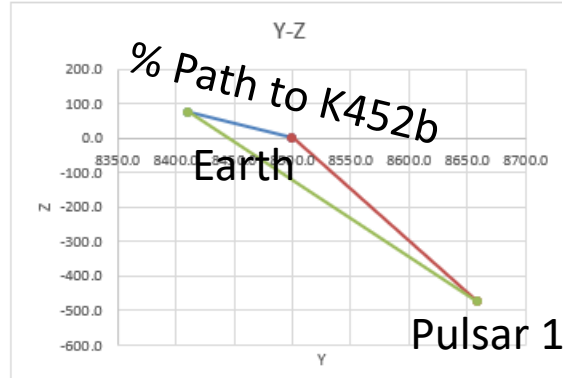

# Model to Calculate Galactic Angles

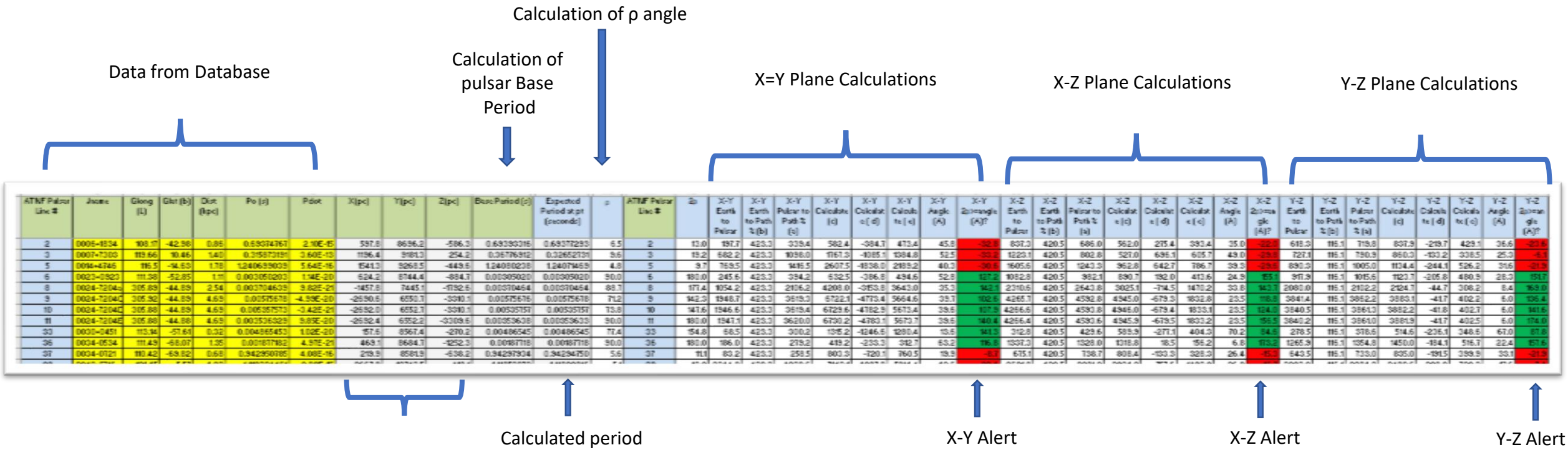

# Pulsars Mapped on the Galactic X-Y Plane

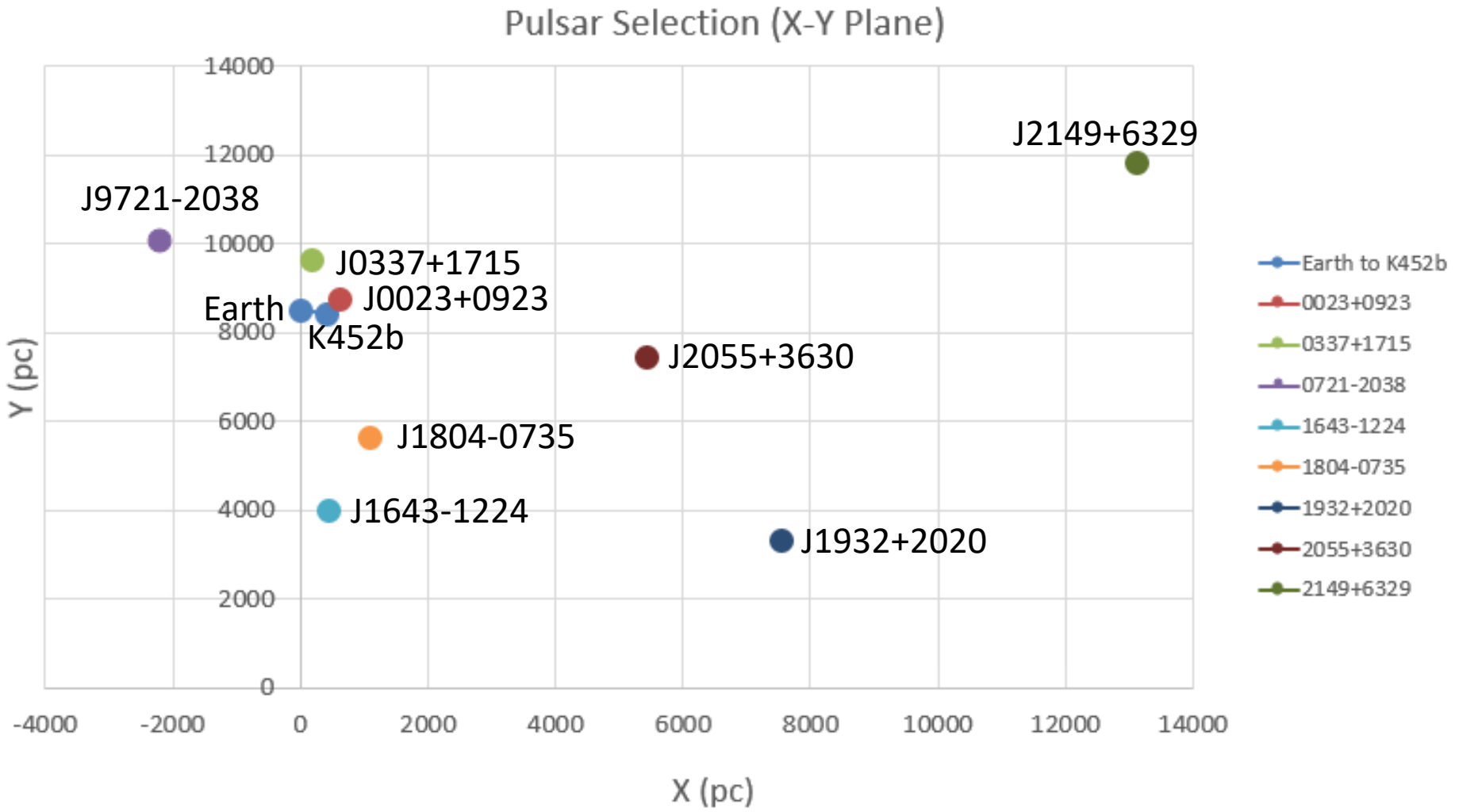

# Solving the 3 Dimensional Position Basic Equations

$$P_{base} = P_{observed} + \dot{P}_{dot}(distance\ in\ light\ years)$$

$$\frac{P_{base1} - P_{observed1}}{\dot{P}_{dot1}} = Pulsar\ 1\ observed\ distance\ \ LY$$

$$\sqrt{(Trial\ X - Pulsar\ 1\ X)^2 + (Trial\ Y - Pulsar\ 1\ Y)^2 + (Trial\ Z - Pulsar\ 1\ Z)^2} = Trial\ Pulsar\ 1\ distance\ (LY)$$

$$\sqrt{(Trial\ X - Pulsar\ 2\ X)^2 + (Trial\ Y - Pulsar\ 2\ Y)^2 + (Trial\ Z - Pulsar\ 2\ Z)^2} = Trial\ Pulsar\ 2\ distance\ (LY)$$

$$\sqrt{(Trial\ X - Pulsar\ 3\ X)^2 + (Trial\ Y - Pulsar\ 3\ Y)^2 + (Trial\ Z - Pulsar\ 3\ Z)^2} = Trial\ Pulsar\ 3\ distance\ (LY)$$

$$\boldsymbol{Pulsar\ 1\ observed\ distance\ (LY) - Trial\ Pulsar\ 1\ distance\ (LY) = delta\ 1}$$

$$\boldsymbol{Pulsar\ 2\ observed\ distance\ (LY) - Trial\ Pulsar\ 2\ distance\ (LY) = delta\ 2}$$

$$\boldsymbol{Pulsar\ 3\ observed\ distance\ (LY) - Trial\ Pulsar\ 3\ distance\ (LY) = delta\ 3}$$

$$\boldsymbol{Solver\ set\ to\ find\ solution\ so\ that: delta\ 1 + delta\ 2 + delta\ 3 = 0}$$

# Solver Model to Calculate Distances

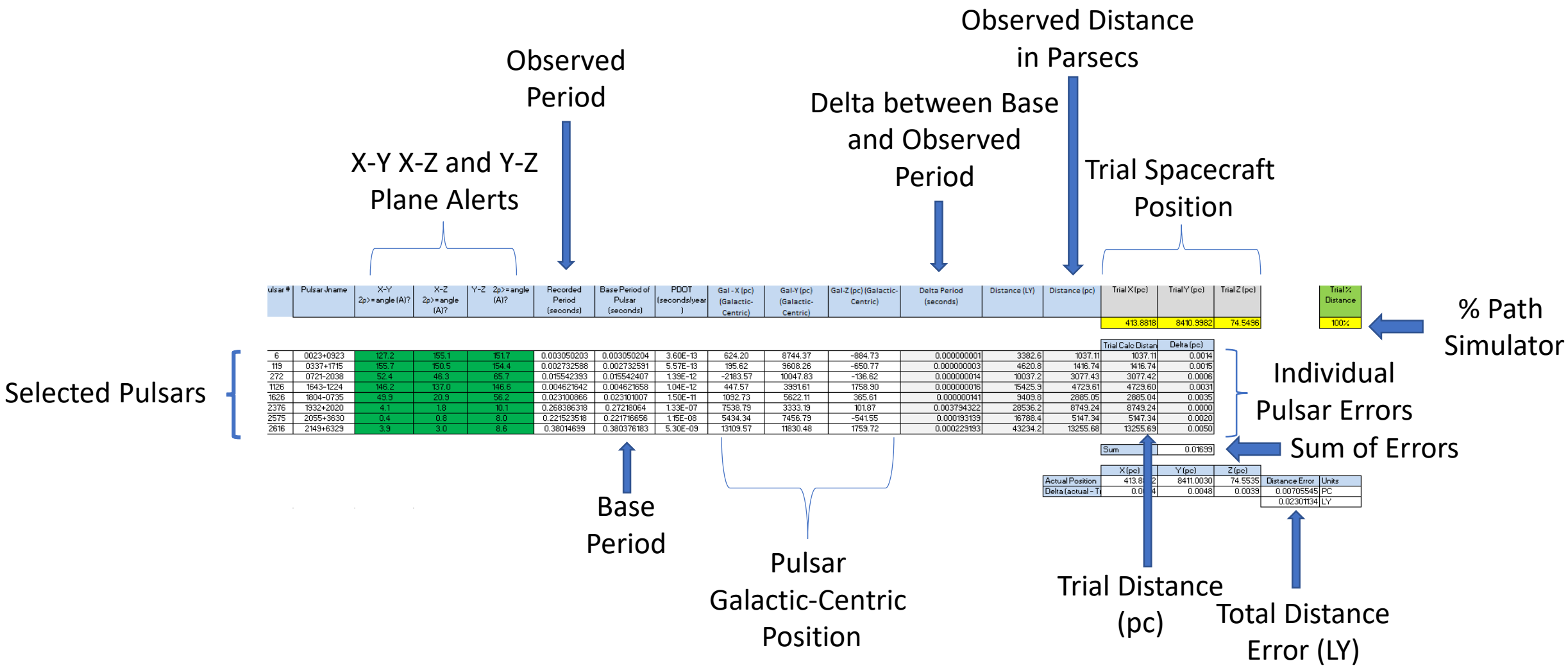


| ulsar # | Pulsar Jname | X-Y 2p>=angle (A)? | X-Z 2p>=angle (A)? | Y-Z 2p>=angle (A)? | Recorded Period (seconds) | Base Period of Pulsar (seconds) | PDOT (seconds/year) | Gal - X (pc) (Galactic-Centric) | Gal-Y (pc) (Galactic-Centric) | Gal-Z (pc) (Galactic-Centric) | Delta Period (seconds) | Distance (LY) | Distance (pc) | Trial X (pc) | Trial Y (pc) | Trial Z (pc) |
|---|---|---|---|---|---|---|---|---|---|---|---|---|---|---|---|---|
| | | | | | | | | | | | | | | 413.8818 | 8410.9382 | 74.5496 |
| 6 | 0023+0923 | 127.2 | 155.1 | 151.7 | 0.003050203 | 0.003050204 | 3.60E-13 | 624.20 | 8744.37 | -884.73 | 0.000000001 | 3382.6 | 1037.11 | 1037.11 | 0.0014 | |
| 119 | 0337+1715 | 155.7 | 150.5 | 154.4 | 0.002732588 | 0.002732591 | 5.57E-13 | 195.62 | 9608.26 | -650.77 | 0.000000003 | 4620.8 | 1416.74 | 1416.74 | 0.0015 | |
| 272 | 0721-2038 | 52.4 | 46.3 | 65.7 | 0.015542393 | 0.015542407 | 1.39E-12 | -2183.57 | 10047.83 | -136.62 | 0.000000014 | 10037.2 | 3077.43 | 3077.42 | 0.0006 | |
| 1126 | 1643-1224 | 146.2 | 137.0 | 146.6 | 0.004621642 | 0.004621658 | 1.04E-12 | 447.57 | 3991.61 | 1758.90 | 0.000000016 | 15425.9 | 4729.61 | 4729.60 | 0.0031 | |
| 1626 | 1804-0735 | 49.9 | 20.9 | 56.2 | 0.023100866 | 0.023101007 | 1.50E-11 | 1092.73 | 5622.11 | 365.61 | 0.000000141 | 9409.8 | 2885.05 | 2885.04 | 0.0035 | |
| 2376 | 1932+2020 | 4.1 | 1.8 | 10.1 | 0.268386318 | 0.27218064 | 1.33E-07 | 7538.79 | 3333.19 | 101.87 | 0.003794322 | 28536.2 | 8749.24 | 8749.24 | 0.0000 | |
| 2575 | 2055+3630 | 0.4 | 0.8 | 8.0 | 0.221523518 | 0.221716656 | 1.15E-08 | 5434.34 | 7456.79 | -541.55 | 0.000193139 | 16788.4 | 5147.34 | 5147.34 | 0.0020 | |
| 2616 | 2149+6329 | 3.9 | 3.0 | 8.6 | 0.38014699 | 0.380376183 | 5.30E-09 | 13109.57 | 11830.48 | 1759.72 | 0.000229193 | 43234.2 | 13255.68 | 13255.69 | 0.0050 | |

| Trial % Distance |
|---|
| 100% |

| | Trial Calc Distan | Delta (pc) |
|---|---|---|
| Sum | | 0.01699 |

| | X (pc) | Y (pc) | Z (pc) | Distance Error | Units |
|---|---|---|---|---|---|
| Actual Position | 413.8 | 8411.0030 | 74.5535 | 0.00705545 | PC |
| Delta (actual - T | 0.0 | 0.0048 | 0.0039 | 0.02301134 | LY |

# Solver Configuration

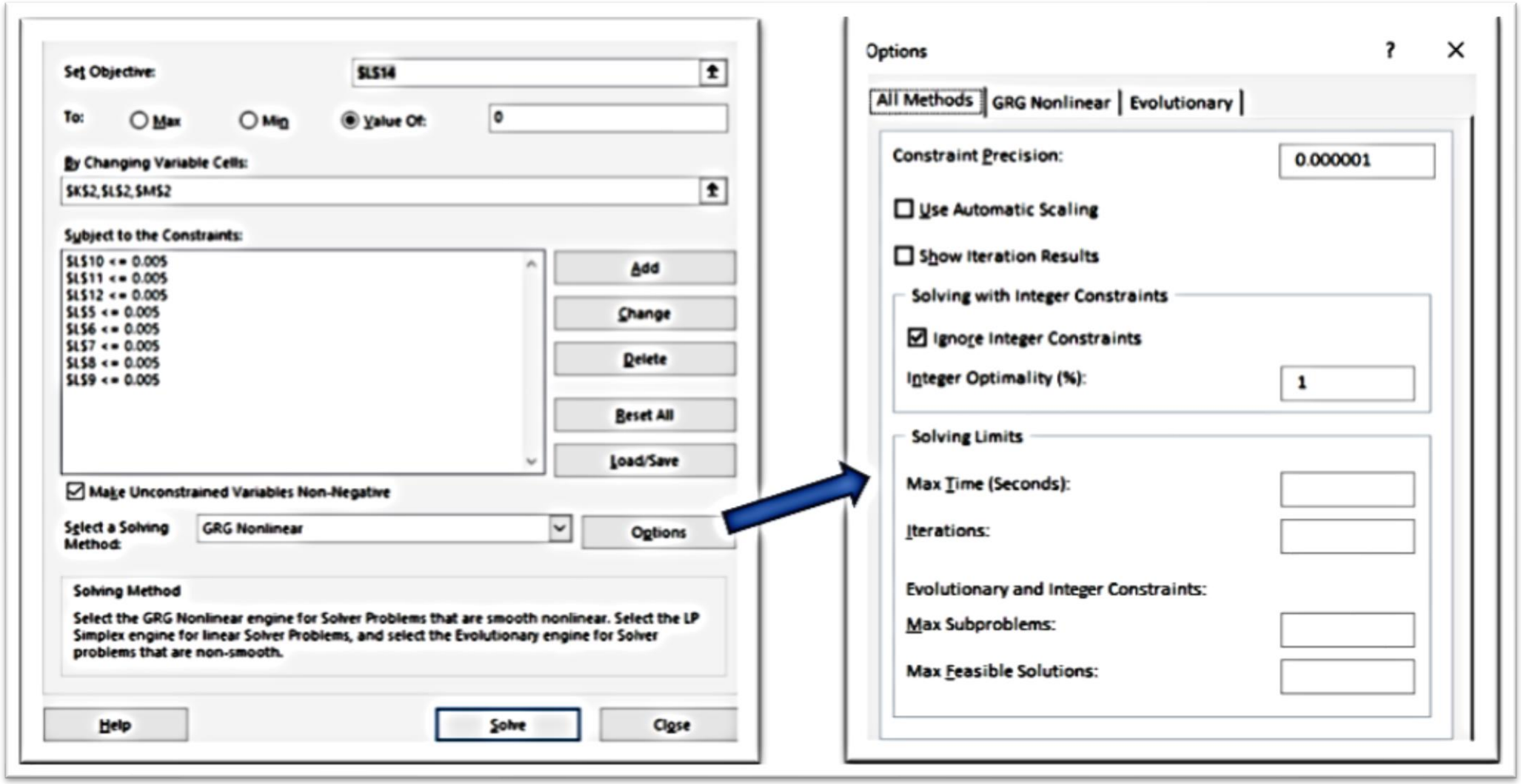

# Solver Error Based on the # of Pulsars Observed

| Trial | % Path Distance | 1 Pulsar Error Analysis (LY) | 2 Pulsar Error Analysis (LY) | 3 Pulsar Error Analysis (LY) | 4 Pulsar Error Analysis (LY) | 5 Pulsar Error Analysis (LY) | 6 Pulsar Error Analysis (LY) | 7 Pulsar Error Analysis (LY) | 8 Pulsar Error Analysis (LY) |
|---|---|---|---|---|---|---|---|---|---|
| 1 | 0% | 225.4768 | 3843.5859 | 0.000001012 | 0.0042 | 0.0002 | 0.0000 | 0.0062 | 0.0087 |
| 2 | 25% | 363.8622 | 3857.0292 | 0.0447 | 0.0212 | 0.3074 | 0.0201 | 0.0262 | 0.0389 |
| 3 | 50% | 559.4236 | 3487.2624 | 0.0437 | 0.0124 | 0.0048 | 0.0323 | 0.0571 | 0.0278 |
| 4 | 75% | 811.1536 | 3103.8657 | 0.0003 | 283.4856 | 0.4195 | 0.0216 | 0.0117 | 0.0116 |
| 5 | 100% | 1129.2855 | 2761.9980 | 0.0508 | 0.0228 | 0.0274 | 0.0300 | 0.0470 | 0.0230 |
| Average | | 617.8404 | 3410.7482 | 0.0279 | 56.7092 | 0.1519 | 0.0208 | 0.0296 | 0.0220 |
| Sigma | | 322.7422 | 426.0101 | 0.0228 | 113.3882 | 0.1766 | 0.0114 | 0.0197 | 0.0110 |

| # of Pulsars used | Average Error (LY) | Standard Deviation (LY) |
|---|---|---|
| 1 | 617.8404 | 322.7422 |
| 2 | 3410.7482 | 426.0101 |
| 3 | 0.0279 | 0.0228 |
| 4 | 56.7092 | 113.3882 |
| 5 | 0.1519 | 0.1766 |
| 6 | 0.0208 | 0.0114 |
| 7 | 0.0296 | 0.0197 |
| 8 | 0.0220 | 0.0110 |

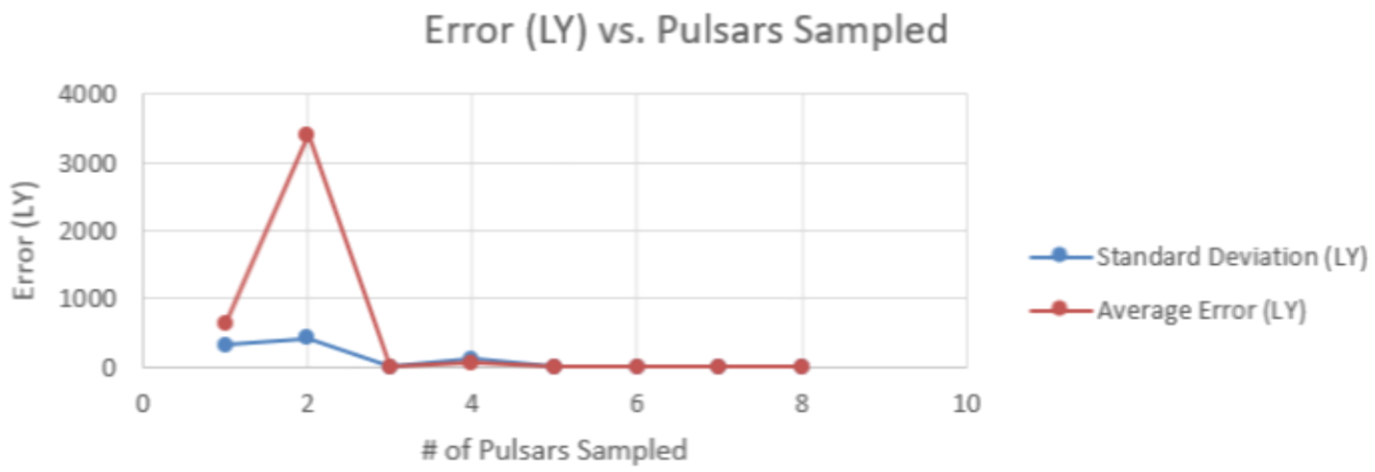

# Is the Error Close Enough?

| Location | Distance From Sun (km) | Distance from Sun (LY) |
|---|---|---|
| Jupiter | 778,000,000 | 0.000082 |
| Pluto | 5,906,376,272 | 0.000624 |
| Edge of Solar System | 9,000,000,000 | 0.000951 |
| 8 Pulsar Error | 208,016,924,775 | 0.021986 |
| Alpha Centauri | 41,345,737,565,365 | 4.370000 |

# Putting it All Together

Navigation Plan for Earth to K452b

# Navigation

**Plan**

- Plot path using galactic coordinates
- Choose pulsars that are visible along entire path

**Underway Observations**

- Stop and take observations
- Calculate new position
- Make course corrections accordingly

# Chart Path using Galactic Coordinates

| | Gal-X (pc) (Galactic-Centric) | Gal-Y (pc) (Galactic-Centric) | Gal-Z (pc) (Galactic-Centric) |
|---|---|---|---|
| Earth | 0.00 | 8500.00 | 0.00 |
| 25% | 103.47 | 8477.75 | 18.64 |
| 50% | 206.94 | 8455.50 | 37.28 |
| 75% | 310.41 | 8433.25 | 55.92 |
| K452b | 413.89 | 8411.00 | 74.55 |

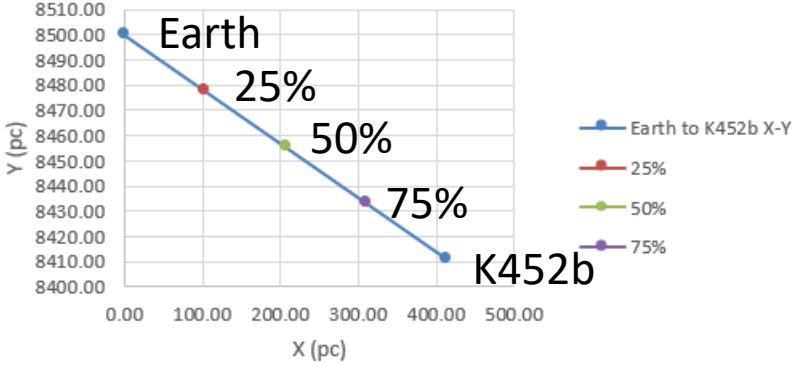


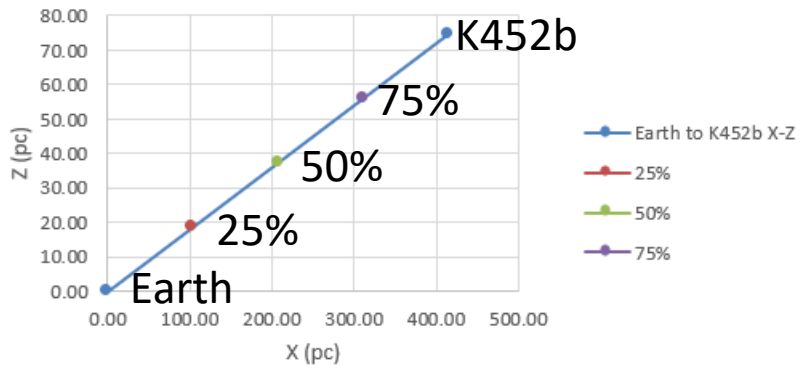


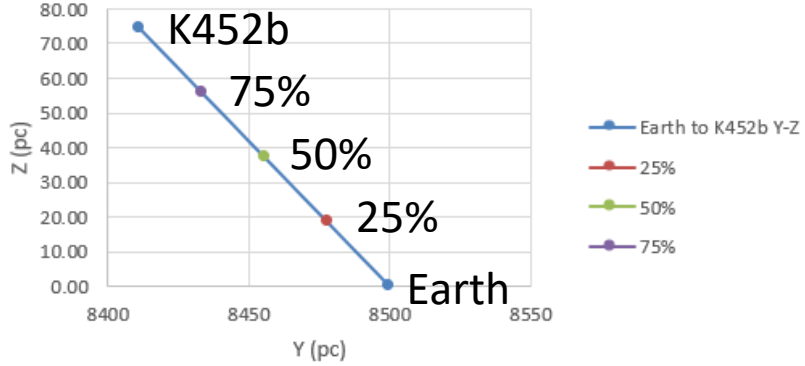

| ATNF Pulsar Line # | Jname | Glong (L) | Glat (b) | Dist (kpc) | Po (s) | Pdot | X(pc) | Y(pc) | Z(pc) | Base Period (s) | Expected Period at pt (seconds) | ρ | ATNF Pulsar Line # | X-Y 2ρ>=angle (A)? | X-Z 2ρ>=angle (A)? | Y-Z 2ρ>=angle (A)? |
|---|---|---|---|---|---|---|---|---|---|---|---|---|---|---|---|---|
| 6 | 0023+0923 | 111.38 | -52.85 | 1.11 | 0.003050203 | 1.14234E-20 | 624.2 | 8744.4 | -884.7 | 0.00305020 | 0.00305020 | 90.0 | 6 | 180.0 | 180.0 | 180.0 |
| 119 | 0337+1715 | 169.99 | -30.04 | 1.30 | 0.002732589 | 1.77E-20 | 195.6 | 9608.3 | -650.8 | 0.00273259 | 0.00273259 | 90.0 | 119 | 180.0 | 180.0 | 180.0 |
| 272 | 0721-2038 | 234.67 | -2.92 | 2.68 | 0.015542395 | 4.40E-20 | -2183.6 | 10047.8 | -136.6 | 0.01554241 | 0.01554239 | 43.3 | 272 | 86.6 | 86.6 | 86.6 |
| 1126 | 1643-1224 | 5.67 | 21.22 | 4.86 | 0.004621641 | 3.30E-20 | 447.6 | 3991.6 | 1758.9 | 0.00462166 | 0.00462164 | 79.4 | 1126 | 158.9 | 158.9 | 158.9 |
| 1626 | 1804-0735 | 20.79 | 6.77 | 3.10 | 0.023100855 | 4.75E-19 | 1092.7 | 5622.1 | 365.6 | 0.02310101 | 0.02310086 | 35.5 | 1626 | 71.1 | 71.1 | 71.1 |
| 2376 | 1932+2020 | 55.57 | 0.64 | 9.14 | 0.268216854 | 4.22E-15 | 7538.8 | 3333.2 | 101.9 | 0.27218064 | 0.26821685 | 10.4 | 2376 | 20.9 | 20.9 | 20.9 |
| 2575 | 2055+3630 | 79.13 | -5.59 | 5.56 | 0.221508034 | 3.65E-16 | 5434.3 | 7456.8 | -541.5 | 0.22171666 | 0.22150803 | 11.5 | 2575 | 22.9 | 22.9 | 22.9 |
| 2616 | 2149+6329 | 104.25 | 7.41 | 13.64 | 0.380140345 | 1.68E-16 | 13109.6 | 11830.5 | 1759.7 | 0.38037618 | 0.38014034 | 8.8 | 2616 | 17.5 | 17.5 | 17.5 |

Earth

| ATNF Pulsar Line # | Jname | Glong (L) | Glat (b) | Dist (kpc) | Po (s) | Pdot | X(pc) | Y(pc) | Z(pc) | Base Period (s) | Expected Period at pt (seconds) | ρ | ATNF Pulsar Line # | X-Y 2ρ>=angle (A)? | X-Z 2ρ>=angle (A)? | Y-Z 2ρ>=angle (A)? |
|---|---|---|---|---|---|---|---|---|---|---|---|---|---|---|---|---|
| 6 | 0023+0923 | 111.38 | -52.85 | 1.11 | 0.003050203 | 1.14234E-20 | 624.2 | 8744.4 | -884.7 | 0.00305020 | 0.00305020 | 90.0 | 6 | 150.8 | 164.4 | 166.7 |
| 119 | 0337+1715 | 169.99 | -30.04 | 1.30 | 0.002732589 | 1.77E-20 | 195.6 | 9608.3 | -650.8 | 0.00273259 | 0.00273259 | 90.0 | 119 | 172.8 | 173.9 | 167.7 |
| 272 | 0721-2038 | 234.67 | -2.92 | 2.68 | 0.015542395 | 4.40E-20 | -2183.6 | 10047.8 | -136.6 | 0.01554241 | 0.01554239 | 43.3 | 272 | 70.8 | 68.4 | 76.5 |
| 1126 | 1643-1224 | 5.67 | 21.22 | 4.86 | 0.004621641 | 3.30E-20 | 447.6 | 3991.6 | 1758.9 | 0.00462166 | 0.00462164 | 79.4 | 1126 | 152.1 | 146.7 | 152.8 |
| 1626 | 1804-0735 | 20.79 | 6.77 | 3.10 | 0.023100855 | 4.75E-19 | 1092.7 | 5622.1 | 365.6 | 0.02310101 | 0.02310086 | 35.5 | 1626 | 60.1 | 46.5 | 63.6 |
| 2376 | 1932+2020 | 55.57 | 0.64 | 9.14 | 0.268216854 | 4.22E-15 | 7538.8 | 3333.2 | 101.9 | 0.27218064 | 0.26825936 | 10.4 | 2376 | 12.5 | 11.3 | 15.5 |
| 2575 | 2055+3630 | 79.13 | -5.59 | 5.56 | 0.221508034 | 3.65E-16 | 5434.3 | 7456.8 | -541.5 | 0.22171666 | 0.22151191 | 11.5 | 2575 | 11.7 | 11.9 | 15.2 |
| 2616 | 2149+6329 | 104.25 | 7.41 | 13.64 | 0.380140345 | 1.68E-16 | 13109.6 | 11830.5 | 1759.7 | 0.38037618 | 0.38014201 | 8.8 | 2616 | 10.7 | 10.3 | 13.1 |

25%

| ATNF Pulsar Line # | Jname | Glong (L) | Glat (b) | Dist (kpc) | Po (s) | Pdot | X(pc) | Y(pc) | Z(pc) | Base Period (s) | Expected Period at pt (seconds) | ρ | ATNF Pulsar Line # | X-Y 2ρ>=angle (A)? | X-Z 2ρ>=angle (A)? | Y-Z 2ρ>=angle (A)? |
|---|---|---|---|---|---|---|---|---|---|---|---|---|---|---|---|---|
| 6 | 0023+0923 | 111.38 | -52.85 | 1.11 | 0.003050203 | 1.14234E-20 | 624.2 | 8744.4 | -884.7 | 0.00305020 | 0.00305020 | 90.0 | 6 | 139.2 | 159.2 | 160.8 |
| 119 | 0337+1715 | 169.99 | -30.04 | 1.30 | 0.002732589 | 1.77E-20 | 195.6 | 9608.3 | -650.8 | 0.00273259 | 0.00273259 | 90.0 | 119 | 167.2 | 170.8 | 162.4 |
| 272 | 0721-2038 | 234.67 | -2.92 | 2.68 | 0.015542395 | 4.40E-20 | -2183.6 | 10047.8 | -136.6 | 0.01554241 | 0.01554239 | 43.3 | 272 | 63.7 | 60.1 | 72.1 |
| 1126 | 1643-1224 | 5.67 | 21.22 | 4.86 | 0.004621641 | 3.30E-20 | 447.6 | 3991.6 | 1758.9 | 0.00462166 | 0.00462164 | 79.4 | 1126 | 149.5 | 142.2 | 150.2 |
| 1626 | 1804-0735 | 20.79 | 6.77 | 3.10 | 0.023100855 | 4.75E-19 | 1092.7 | 5622.1 | 365.6 | 0.02310101 | 0.02310086 | 35.5 | 1626 | 55.7 | 36.1 | 60.5 |
| 2376 | 1932+2020 | 55.57 | 0.64 | 9.14 | 0.268216854 | 4.22E-15 | 7538.8 | 3333.2 | 101.9 | 0.27218064 | 0.26830178 | 10.4 | 2376 | 9.0 | 7.4 | 13.3 |
| 2575 | 2055+3630 | 79.13 | -5.59 | 5.56 | 0.221508034 | 3.65E-16 | 5434.3 | 7456.8 | -541.5 | 0.22171666 | 0.22151579 | 11.5 | 2575 | 7.1 | 7.3 | 12.1 |
| 2616 | 2149+6329 | 104.25 | 7.41 | 13.64 | 0.380140345 | 1.68E-16 | 13109.6 | 11830.5 | 1759.7 | 0.38037618 | 0.38014367 | 8.8 | 2616 | 7.9 | 7.3 | 11.3 |

50%

| ATNF Pulsar Line # | Jname | Glong (L) | Glat (b) | Dist (kpc) | Po (s) | Pdot | X(pc) | Y(pc) | Z(pc) | Base Period (s) | Expected Period at pt (seconds) | ρ | ATNF Pulsar Line # | X-Y 2ρ>=angle (A)? | X-Z 2ρ>=angle (A)? | Y-Z 2ρ>=angle (A)? |
|---|---|---|---|---|---|---|---|---|---|---|---|---|---|---|---|---|
| 6 | 0023+0923 | 111.38 | -52.85 | 1.11 | 0.003050203 | 1.14234E-20 | 624.2 | 8744.4 | -884.7 | 0.00305020 | 0.00305020 | 90.0 | 6 | 131.2 | 156.3 | 156.0 |
| 119 | 0337+1715 | 169.99 | -30.04 | 1.30 | 0.002732589 | 1.77E-20 | 195.6 | 9608.3 | -650.8 | 0.00273259 | 0.00273259 | 90.0 | 119 | 161.5 | 160.6 | 158.2 |
| 272 | 0721-2038 | 234.67 | -2.92 | 2.68 | 0.015542395 | 4.40E-20 | -2183.6 | 10047.8 | -136.6 | 0.01554241 | 0.01554239 | 43.3 | 272 | 57.8 | 53.0 | 68.7 |
| 1126 | 1643-1224 | 5.67 | 21.22 | 4.86 | 0.004621641 | 3.30E-20 | 447.6 | 3991.6 | 1758.9 | 0.00462166 | 0.00462164 | 79.4 | 1126 | 147.6 | 139.1 | 148.3 |
| 1626 | 1804-0735 | 20.79 | 6.77 | 3.10 | 0.023100855 | 4.75E-19 | 1092.7 | 5622.1 | 365.6 | 0.02310101 | 0.02310086 | 35.5 | 1626 | 52.5 | 28.0 | 58.2 |
| 2376 | 1932+2020 | 55.57 | 0.64 | 9.14 | 0.268216854 | 4.22E-15 | 7538.8 | 3333.2 | 101.9 | 0.27218064 | 0.26834410 | 10.4 | 2376 | 6.3 | 4.3 | 11.6 |
| 2575 | 2055+3630 | 79.13 | -5.59 | 5.56 | 0.221508034 | 3.65E-16 | 5434.3 | 7456.8 | -541.5 | 0.22171666 | 0.22151966 | 11.5 | 2575 | 3.4 | 3.8 | 9.8 |
| 2616 | 2149+6329 | 104.25 | 7.41 | 13.64 | 0.380140345 | 1.68E-16 | 13109.6 | 11830.5 | 1759.7 | 0.38037618 | 0.38014533 | 8.8 | 2616 | 5.8 | 5.0 | 9.8 |

75%

| ATNF Pulsar Line # | Jname | Glong (L) | Glat (b) | Dist (kpc) | Po (s) | Pdot | X(pc) | Y(pc) | Z(pc) | Base Period (s) | Expected Period at pt (seconds) | ρ | ATNF Pulsar Line # | X-Y 2ρ>=angle (A)? | X-Z 2ρ>=angle (A)? | Y-Z 2ρ>=angle (A)? |
|---|---|---|---|---|---|---|---|---|---|---|---|---|---|---|---|---|
| 6 | 0023+0923 | 111.38 | -52.85 | 1.11 | 0.003050203 | 1.14234E-20 | 624.2 | 8744.4 | -884.7 | 0.00305020 | 0.00305020 | 90.0 | 6 | 126.0 | 155.1 | 151.7 |
| 119 | 0337+1715 | 169.99 | -30.04 | 1.30 | 0.002732589 | 1.77E-20 | 195.6 | 9608.3 | -650.8 | 0.00273259 | 0.00273259 | 90.0 | 119 | 155.7 | 150.5 | 154.4 |
| 272 | 0721-2038 | 234.67 | -2.92 | 2.68 | 0.015542395 | 4.40E-20 | -2183.6 | 10047.8 | -136.6 | 0.01554241 | 0.01554239 | 43.3 | 272 | 52.4 | 46.3 | 65.7 |
| 1126 | 1643-1224 | 5.67 | 21.22 | 4.86 | 0.004621641 | 3.30E-20 | 447.6 | 3991.6 | 1758.9 | 0.00462166 | 0.00462164 | 79.4 | 1126 | 146.2 | 137.0 | 146.6 |
| 1626 | 1804-0735 | 20.79 | 6.77 | 3.10 | 0.023100855 | 4.75E-19 | 1092.7 | 5622.1 | 365.6 | 0.02310101 | 0.02310087 | 35.5 | 1626 | 49.9 | 20.9 | 56.2 |
| 2376 | 1932+2020 | 55.57 | 0.64 | 9.14 | 0.268216854 | 4.22E-15 | 7538.8 | 3333.2 | 101.9 | 0.27218064 | 0.26838632 | 10.4 | 2376 | 4.1 | 1.8 | 10.1 |
| 2575 | 2055+3630 | 79.13 | -5.59 | 5.56 | 0.221508034 | 3.65E-16 | 5434.3 | 7456.8 | -541.5 | 0.22171666 | 0.22152352 | 11.5 | 2575 | 0.4 | 0.8 | 8.0 |
| 2616 | 2149+6329 | 104.25 | 7.41 | 13.64 | 0.380140345 | 1.68E-16 | 13109.6 | 11830.5 | 1759.7 | 0.38037618 | 0.38014699 | 8.8 | 2616 | 3.9 | 3.0 | 8.6 |

K452b

Select Pulsars that are visible along entire path

# Take Pulsar Observations at the 25% Path Point then use the solver to determine the galactic position

## Observed Pulsar periods

| Pulsar # | Pulsar Jname | Recorded Period (seconds) |
|---|---|---|
| 6 | 0023+0923 | 0.003050203 |
| 119 | 0337+1715 | 0.002732589 |
| 272 | 0721-2038 | 0.015542394 |
| 1126 | 1643-1224 | 0.004621642 |
| 1626 | 1804-0735 | 0.023100858 |
| 2376 | 1932+2020 | 0.268269331 |
| 2575 | 2055+3630 | 0.22151318 |
| 2616 | 2149+6329 | 0.380142661 |

## Solver Solution

| Trial X (pc) | Trial Y (pc) | Trial Z (pc) |
|---|---|---|
| 139.9948 | 8489.9997 | 15.0002 |

| Pulsar # | Pulsar Jname | Recorded Period (seconds) | Base Period of Pulsar (seconds) | PDOT (seconds/year) | Gal - X (pc) (Galactic-Centric) | Gal-Y (pc) (Galactic-Centric) | Gal-Z (pc) (Galactic-Centric) | Delta Period (seconds) | Distance (LY) | Distance (pc) | Trial X (pc) | Trial Y (pc) | Trial Z (pc) |
|---|---|---|---|---|---|---|---|---|---|---|---|---|---|
| | | | | | | | | | | | 139.9948 | 8489.9997 | 15.0002 |
| | | | | | | | | | | | | Trial Calc Dista | Delta (pc) |
| 6 | 0023+0923 | 0.003050203 | 0.003050204 | 3.60E-13 | 624.20 | 8744.37 | -884.73 | 0.000000001 | 3434.2 | 1052.94 | 1052.94 | 0.0026 | |
| 119 | 0337+1715 | 0.002732589 | 0.002732591 | 5.57E-13 | 195.62 | 9608.26 | -650.77 | 0.000000002 | 4248.6 | 1302.63 | 1302.63 | 0.0006 | |
| 272 | 0721-2038 | 0.015542394 | 0.015542407 | 1.39E-12 | -2183.57 | 10047.83 | -136.62 | 0.000000013 | 9137.5 | 2801.57 | 2801.56 | 0.0041 | |
| 1126 | 1643-1224 | 0.004621642 | 0.004621658 | 1.04E-12 | 447.57 | 3991.61 | 1758.90 | 0.000000016 | 15767.7 | 4834.38 | 4834.38 | 0.0000 | |
| 1626 | 1804-0735 | 0.023100858 | 0.023101007 | 1.50E-11 | 1092.73 | 5622.11 | 365.61 | 0.000000149 | 9922.6 | 3042.27 | 3042.28 | 0.0013 | |
| 2376 | 1932+2020 | 0.268269331 | 0.27218064 | 1.33E-07 | 7538.79 | 3333.19 | 101.87 | 0.003911309 | 29416.0 | 9019.00 | 9019.00 | 0.0041 | |
| 2575 | 2055+3630 | 0.22151318 | 0.221716656 | 1.15E-08 | 5434.34 | 7456.79 | -541.55 | 0.000203477 | 17687.0 | 5422.85 | 5422.85 | 0.0050 | |
| 2616 | 2149+6329 | 0.380142661 | 0.380376183 | 5.30E-09 | 13109.57 | 11830.48 | 1759.72 | 0.000233522 | 44050.8 | 13506.02 | 13506.03 | 0.0050 | |
| | | | | | | | | | | | Sum | 0.02266 | |

# Position Error in X-Y Plane

Solver position based
on observed periods at 25% point

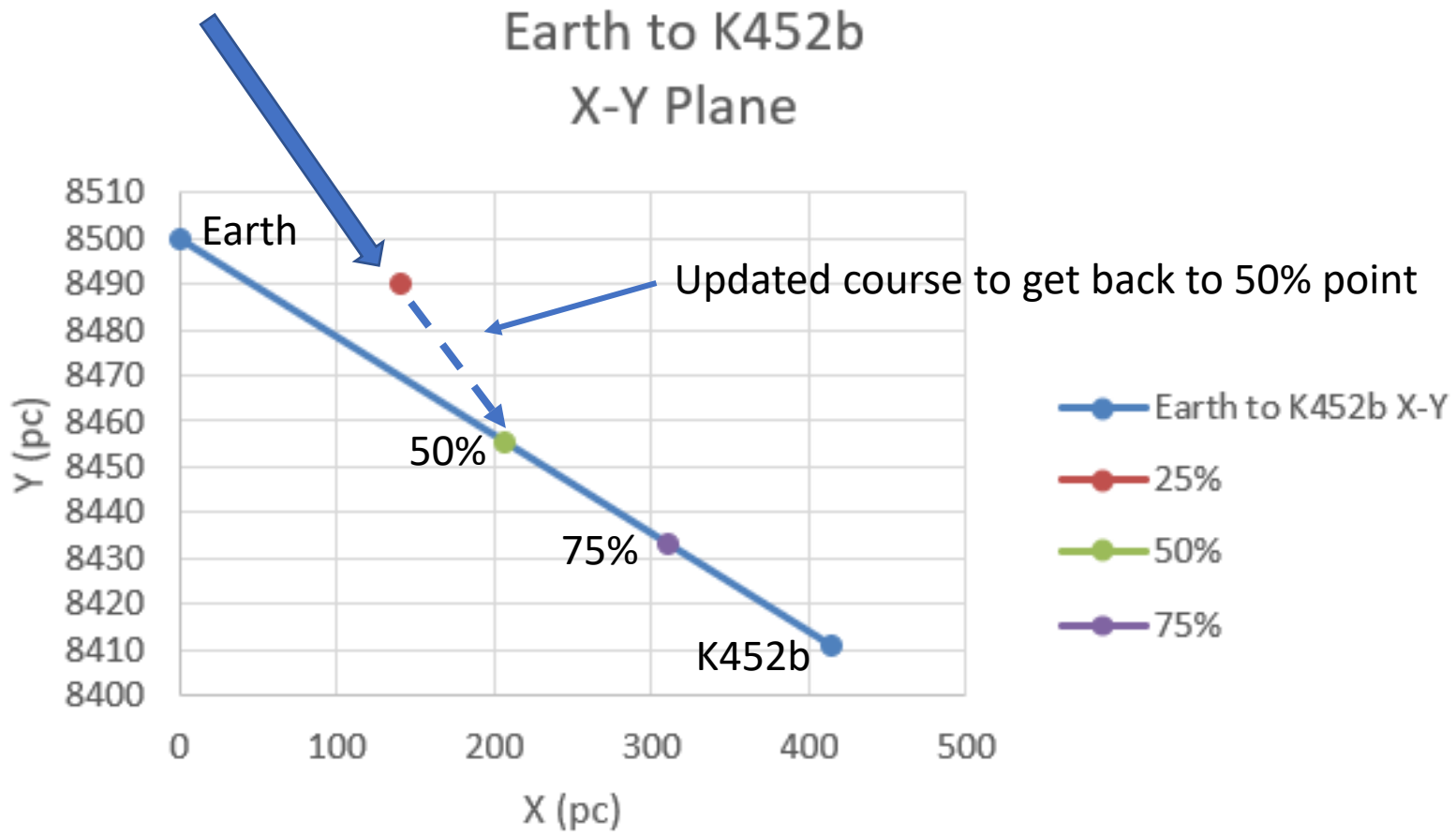

# Required Course Updates
# All 3 Planes

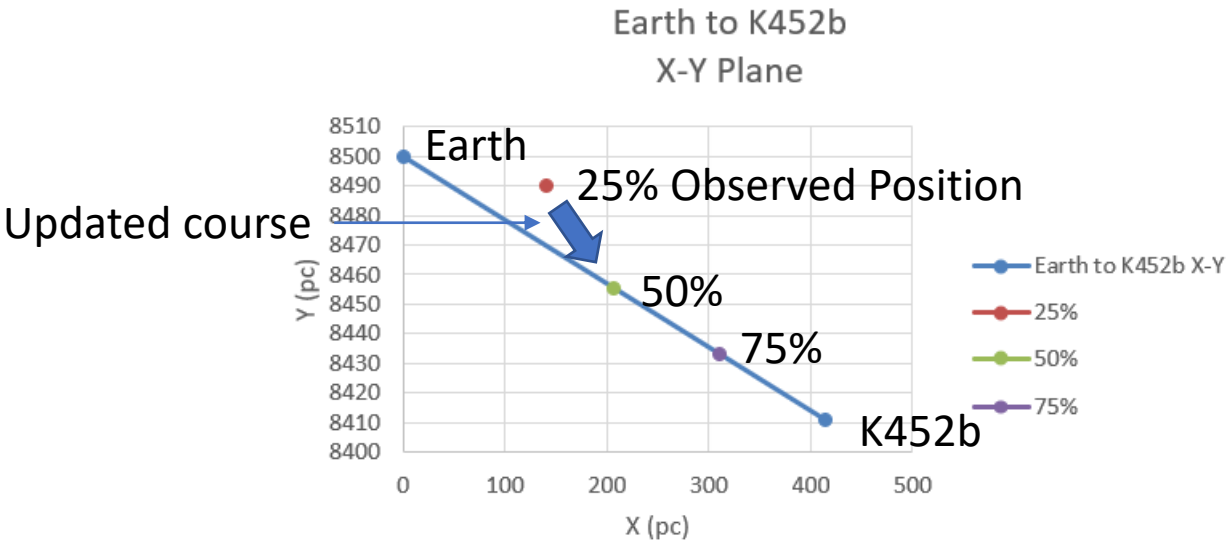


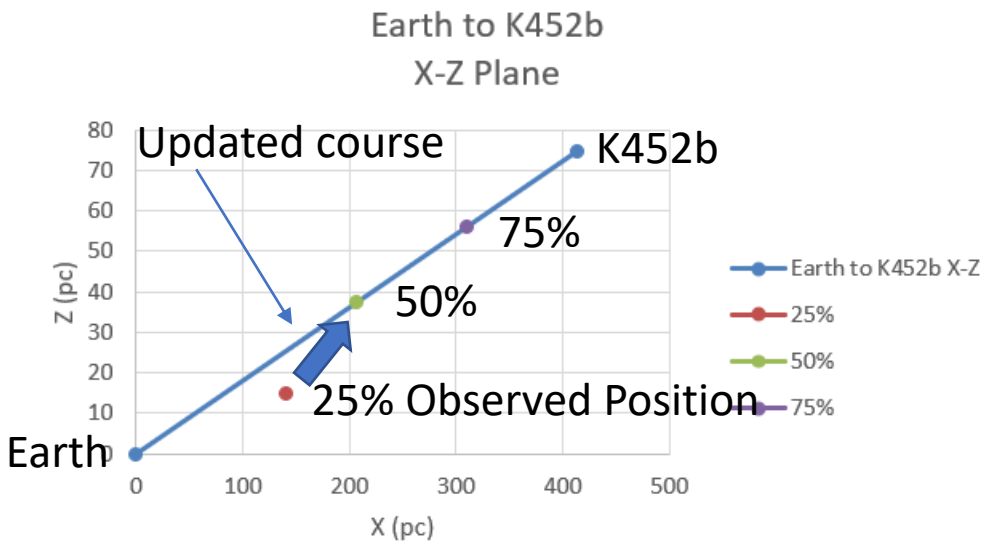


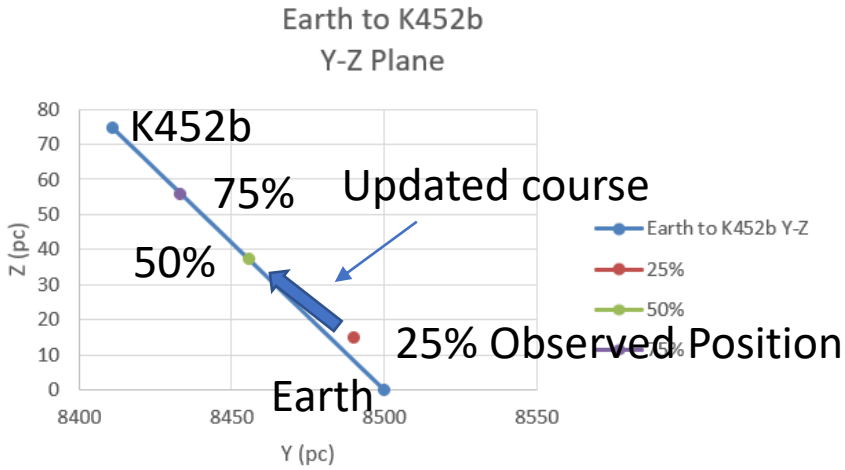

# Summary

- Pulsars can provide reasonable navigation accuracy for galactic flight
- Errors can be reduced by using a better “solver” than Excel
- We should be able to see the Earth position change using this method

- SETI
  - Transmitting the binary code for 3 pulsars would provide our unique position in the galaxy
  - Transmitting more than 3 pulsars would account for visibility angles of the ETI